Journal of Power Sources 195 (2010) 2928–2934

Contents lists available at ScienceDirect

Journal of Power Sources

journal homepage: www.elsevier.com/locate/jpowsour

Short communication

Preparation of electrochemically active lithium sulfide–carbon composites using spark-plasma-sintering process

Tomonari Takeuchi*, Hikari Sakaebe, Hiroyuki Kageyama, Hiroshi Senoh, Tetsuo Sakai, Kuniaki Tatsumi

National Institute of Advanced Industrial Science and Technology (AIST), Midorigaoka 1-8-31, Ikeda, Osaka, 563-8577, Japan

ARTICLE INFO

Article history:
Received 23 August 2009
Received in revised form 30 October 2009
Accepted 2 November 2009
Available online 10 November 2009

Keywords:
Lithium sulfide
Carbon composite
Positive electrode
Lithium-ion battery
Spark-plasma-sintering process

ABSTRACT

Electrochemically active lithium sulfide–carbon (Li_2S–C) composite positive electrodes, applicable for rechargeable lithium-ion batteries, were prepared using spark-plasma-sintering (SPS) process. The electrochemical tests demonstrated that the SPS-treated Li_2S–C composites showed the initial charge and discharge capacities of *ca.* 1200 and 200 mAh g^{-1}, respectively, though Li_2S has been reported to show no significant charge capacities when conventionally mixed with carbon powder. Such activation of Li_2S was attributed principally to strong bindings between Li_2S and carbon powders, formed by the SPS treatment. The *ex situ* XRD measurements showed that some amounts of Li_2S were still remained unchanged and any elemental sulfur was not detected even at fully charged state, which was similar to Li/S cells.

1. Introduction

Sulfur-based materials are promising cathode active materials for high-energy rechargeable lithium batteries because of their high theoretical capacities and relatively low costs [1–6]. For example, elemental sulfur has the theoretical specific capacity of *ca.* 1670 mAh g^{-1}, and a Li/S redox couple could generate the energy density of *ca.* 2600 Wh kg^{-1}, which is much higher than those of the currently available systems with oxide-based cathodes, such as $LiC_6/LiCoO_2$ and $Li/LiMn_2O_4$ (theoretically *ca.* 430–570 Wh kg^{-1}, practically *ca.* 120–180 Wh kg^{-1}) [1,5]. Lithium sulfide (Li_2S) also has a high theoretical capacity (*ca.* 1170 mAh g^{-1}) and has an advantage that a variety of anode materials without lithium sources are applicable in the practical battery system [6]. However, Li_2S, as well as elemental sulfur, is both electronically and ionically resistive, which gives rise to low active material utilization in the cells. Indeed, Obrovac and Dahn reported that Li_2S electrode cells showed no significant capacity when charged to 4.8 V [4], and Jeon et al. reported that no oxidation peak was present up to 3 V in the Li/Li_2S cells [7].

Several attempts have been performed to enhance the conductivity of Li_2S, such as forming the composites with several metals (Li_2S–Fe, Li_2S–Cu) [4,6]. These composites have an advantage that metal sulfides (FeS, CuS), formed during the electrochemical reactions of the cells, also act as active materials, and it contributes to enlarge the capacity of the cathode materials. On the other hand, forming the composites with carbon (Li_2S–C) is an alternative approach to enhance the conductivity of Li_2S. This method is advantageous for prevailing the additive conducting materials more homogeneously inside the positive electrodes, because of the availability of fine carbon powders, and is also advantageous from the standpoint of lower cost of carbon. Although there have been several attempts to prepare S–C composites, such as a vapor deposition of elemental sulfur on fine carbon powders [5,8,9], very few approaches were reported for the Li_2S–C composites. This would be partly because of the less variety of methods applicable for preparing the Li_2S–C composites under inert (or reductive) atmosphere. In addition, carbon composites usually reduce the density of the electrodes due to the bulky volume of carbon, which leads to the decrease in battery energy density per volume [10]. Therefore, a method to form Li_2S–C composites without reducing the density is required.

Spark-plasma-sintering (SPS) is a process that makes use of microscopic electrical discharge between particles [11]. In this process, the powders loaded in the graphite die are pressed uniaxially (*ca.* 30–50 MPa), and a pulsed DC current (*ca.* 1000 A) is simultaneously applied to generate a spark discharge between particles, which generates an internal localized heating, promotes material transfer, accelerates the contacts between particles, and results in producing dense polycrystalline microstructures within a very short time (typically several minutes) [11,12]. Recently, we have applied this method to $LiFePO_4$ + C, $LiMn_2O_4$ + C, and $Li(Ni,Co)O_2$ + C as an attempt to form strong binding between the active materials and carbon powders, and it was successful to form the dense

* Corresponding author. Tel.: +81 72 751 9618; fax: +81 72 751 9714.
E-mail address: takeuchi.tomonari@aist.go.jp (T. Takeuchi).

0378-7753/$ – see front matter © 2009 Elsevier B.V. All rights reserved.
doi:10.1016/j.jpowsour.2009.11.011

composites with well-developed electrical networks, which resulted in the improvement of the electrode density and the electrochemical performances [13–15]. As compared to the oxide-based active materials, Li_2S would be favorable for the SPS process, because the decomposition under the reductive SPS conditions seems to be much less.

In the present work, we tried to improve the utilization of Li_2S by forming the composites with carbon powders using the SPS process. The electrochemical properties, morphologies, and the tap densities of the resulting Li_2S–C composites were examined, and the charge/discharge mechanisms of Li_2S itself in the cells with liquid electrolytes were investigated.

2. Experimental

Since Li_2S is very sensitive to moisture and oxygen, most of the procedures were carried out in an argon-filled glove box. The Li_2S–C composites were prepared by the following SPS procedure: the commercially available Li_2S (Mitsuwa Chemicals, Japan) was blended thoroughly with acetylene black (AB) powder in an 8:2 weight ratio using a ball-milling process, and the mixture was then placed in a graphite die (15 mm diameter). After the graphite die was equipped in the SPS apparatus (SPS-3.20 MK-IV, SPS Syntex Inc., Japan), the system was evacuated down to *ca.* 20 Pa and then filled with argon gas, followed by applying a DC electric current of 400–1000 A to pass through the graphite die. During this procedure, the temperature was increased to 400–1000 °C at a rate of 200 °C min^{-1} (controlled by the applied current). After it attained to a given temperature, the current was switched off and the sample was cooled to room temperature, then the Li_2S–C composite samples were obtained.

The phase purity of the samples was checked by X-ray diffraction (XRD) measurements (Rotaflex RU-200B/RINT, Rigaku, Japan) using monochromatic Cu Kα radiation within the 2θ range of 10–125°. The RIETAN-2000 program was used for structural refinement with X-ray Rietveld analysis [16]. Morphology of the samples was examined by scanning electron microscopy (SEM; JEOL JSM-5500LV). The particle size distribution of the powder samples was measured by laser diffraction and scattering method (AEROTRAC SPR, Model No. 7340, Nikkiso). The tap density was estimated from the sample weight and the volume in the measuring cylinder after tapping several tens times. The electrochemical lithium extraction/insertion reactions were carried out using lithium coin-type cells. The working electrode consisted of a mixture of a 12 mg Li_2S–C composite and a 0.5 mg Teflon powder pressed into a 15 mm diameter tablet under a pressure of 10 MPa. The electrochemical test cells were constructed in a stainless steel coin-type configuration. The negative electrode was a 15 mm diameter and 0.2 mm thick disk of Li foil, and the separator was a microporous polyolefin sheet. The solution of 1 M lithium bis(trifluoro-methanesulfonyl) imide (LiTFSI, $LiN(CF_3SO_2)_2$) in tetra(ethylene glycol) dimethylether (TEGDME, $CH_3(OCH_2CH_2)_4OCH_3$) was used as the electrolyte. The electrochemical measurements were carried out at 30 °C initially with charging, after standing overnight on open circuit, using a TOSCAT-3100 (Toyo System, Japan) at a current density of 46.7 mA g^{-1} (0.04 C) between 3.0 and 1.3 V. The impedance of the cells was measured using a frequency response analyzer (SI 1260, Solartron Analytical) and a potentiostat (model 263A, Princeton Applied Research), covering a frequency range of 0.1 Hz to 100 kHz with an applied voltage of 10 mV.

3. Results and discussion

The SPS-treated Li_2S–C composites were black in color, and the appearance was similar to that of the Li_2S + C blended powder.

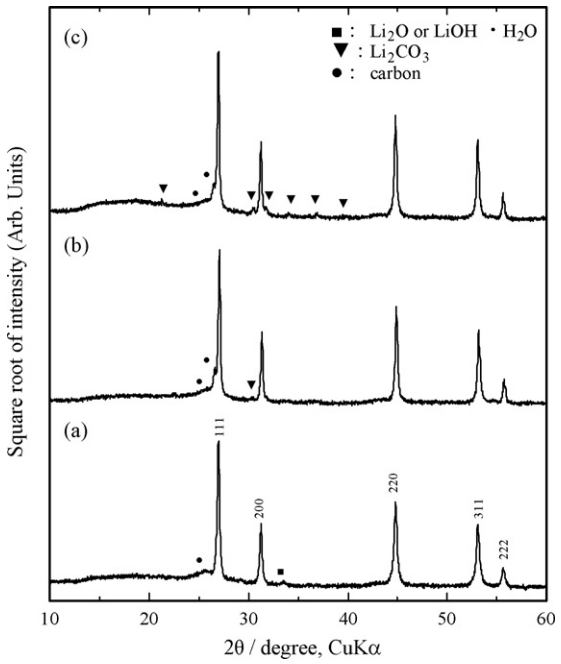

Fig. 1. XRD patterns (Cu Kα radiation) for (a) the Li_2S + C blended powder and the SPS-treated ((b) at 600 °C and (c) 1000 °C) Li_2S–C composites.

Fig. 1 shows the XRD patterns for the Li_2S + C blended powder and the SPS-treated (at 600 and 1000 °C) Li_2S–C composite samples. Most of the peaks were indexed by the cubic unit cell ($Fm\bar{3}m$), and the estimated lattice parameters (a = 5.70875(12)–5.71515(11) Å) were consistent with that (a = 5.7158(1) Å) reported previously for Li_2S [17]. Small peaks (denoted as closed squares), which were assigned to Li_2O or $LiOH{\cdot}H_2O$, were detected in the Li_2S + C blended powder, and they disappeared after the SPS treatment. In addition, other small peaks (denoted as closed triangles), which were assigned to Li_2CO_3, were observed in the Li_2S–C composites, particularly those treated at higher SPS temperatures. Small peaks located at around 2θ = 26° are assigned to carbon; a broad peak at 2θ = 25.5° is originated from the acetylene black, and a sharp peak at 2θ = 26.5° is from the graphite contaminated from the die during the SPS process. The sample weights were nearly unchanged during the present SPS process (for example, the initial sample weight was reduced by *ca.* 2.6% after the SPS-1000 °C-treatment), therefore the carbon contents in the composite samples were remained to *ca.* 20%.

Along with the appearance of these impurities, the lattice parameter of Li_2S showed a slight change; the a-value shows a minimum at 600 °C-treated samples, as shown in Fig. 2. According to the previous reports [17,18], the lattice parameter of Li_2S increases with the decrease in occupancy of lithium at 8c site in a cubic unit cell $[Li_{2x}]_{8c}[S]_{4a}$ ($0 < x < 1$). Therefore, the lithium deficiency of Li_2S in the SPS-composites might be minimized in the 600 °C-treated samples. Although the x-value cannot be estimated from the analysis of XRD data because of very little contribution to the diffraction intensity from lithium atoms, we tried to calculate the x-value by the X-ray Rietveld analysis [16], assuming that the lithium deficiency would result in the slight rearrangements of sulfur atoms and it would affect the intensity of the XRD peaks. The calculated x-value, Fig. 2, shows a maximum at 600–800 °C-treated samples, and it is approximately consistent with the above speculation that the lithium deficiency of Li_2S was minimized in the 600 °C-treated SPS composites. The error bars in x-values signify the distribution of the lithium deficiency of Li_2S in the composite samples. These observations suggest that the Li_2O (or $LiOH{\cdot}H_2O$) in

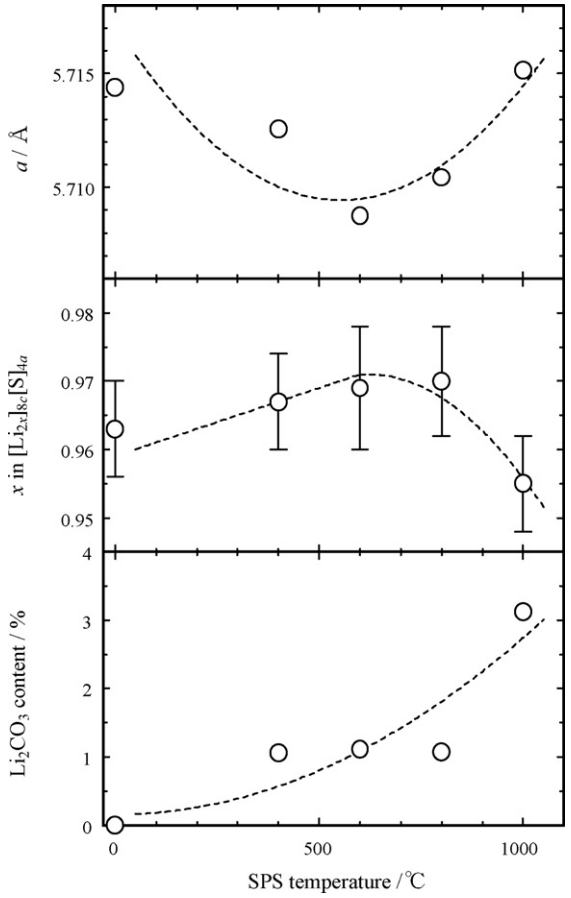

Fig. 2. Lattice parameter (a/Å), lithium occupancy at 8c site (x in $[Li_{2x}]_{8c}[S]_{4a}$), and Li_2CO_3 content, estimated by the X-ray Rietveld analyses, for the Li_2S–C composites as a function of SPS temperature.

the Li_2S + C blended powder, probably formed by the partial decomposition of Li_2S due to the presence of trace amounts of air during the ball-milling process, was reduced and again incorporated into Li_2S during the SPS process, resulting in the decrease in lithium deficiency of Li_2S. Of course, there is a possibility that some oxide-based amorphous compounds were formed by the SPS treatment, but the amounts of such amorphous phases, if any, would be much less than *ca.* 1%, because the amount of Li_2O (or $LiOH{\cdot}H_2O$) in the Li_2S + C blended powder was estimated to be less than 1% by the X-ray Rietveld analyses [16], which would give rise to little influence on the properties, such as the electrochemical performances, of the composite samples. Fig. 2 also shows the calculated Li_2CO_3 contents (in weight%) estimated by the X-ray Rietveld analyses [16]. At higher SPS temperatures, decomposition of Li_2S proceeded and Li_2CO_3 was formed, probably by the reaction with trace amounts of air and carbon powder, resulting in the increase in lithium deficiency of Li_2S. Such decomposition became significant above 1000 °C, as shown in Fig. 2. Thus, the 600 °C-treated SPS composites have less amounts of impurity and would have less lithium deficiency in Li_2S.

Fig. 3 shows typical SEM micrographs of the Li_2S + C blended powder and the SPS-treated (at 600 and 1000 °C) Li_2S–C composite samples. The Li_2S + C blended powder consisted of mainly several micrometer-sized particles with rather homogeneous distribution. On the other hand, the SPS-treated Li_2S–C composites consisted of agglomerates with the size of >10 μm, where Li_2S particles seemed to be connected each other via carbon particles. Indeed, magnified SEM images, Fig. 4(b) and (c), indicate that the carbon particles were rather embedded homogeneously in the Li_2S particles connected

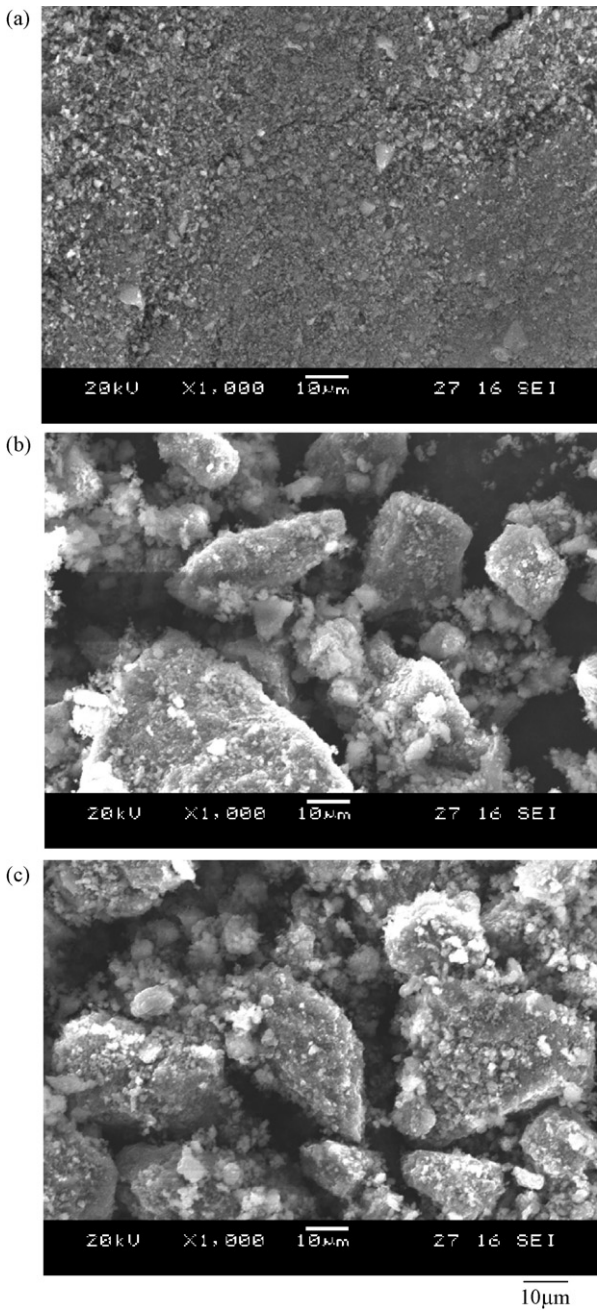

Fig. 3. SEM images of (a) the Li_2S + C blended powder and the SPS-treated ((b) at 600 °C and (c) 1000 °C) Li_2S–C composites. Magnification is the same for each micrograph.

strongly each other, signifying the formation of strong binding among the Li_2S and carbon particles. This makes a clear contrast to the Li_2S + C blended powder, Fig. 4(a), where the carbon particles were just loaded subtly on the Li_2S particles inhomogeneously, and there observed several smooth surfaces of Li_2S particles, not covered with carbon powder.

These SEM observations were consistent with the particle size distribution measured by laser diffraction and scattering method, Fig. 5. The Li_2S + C blended powder consisted of 0.5–20 μm particles, and the average particle size, represented by the value at 50% cumulative population ($d_{50\%}$), was 3.0 μm. After the SPS treatment, the population of larger particles of >10 μm drastically increased, resulting in larger $d_{50\%}$ values (10.6–12.2 μm), which is consistent with the presence of agglomerates of >10 μm in SEM observations.

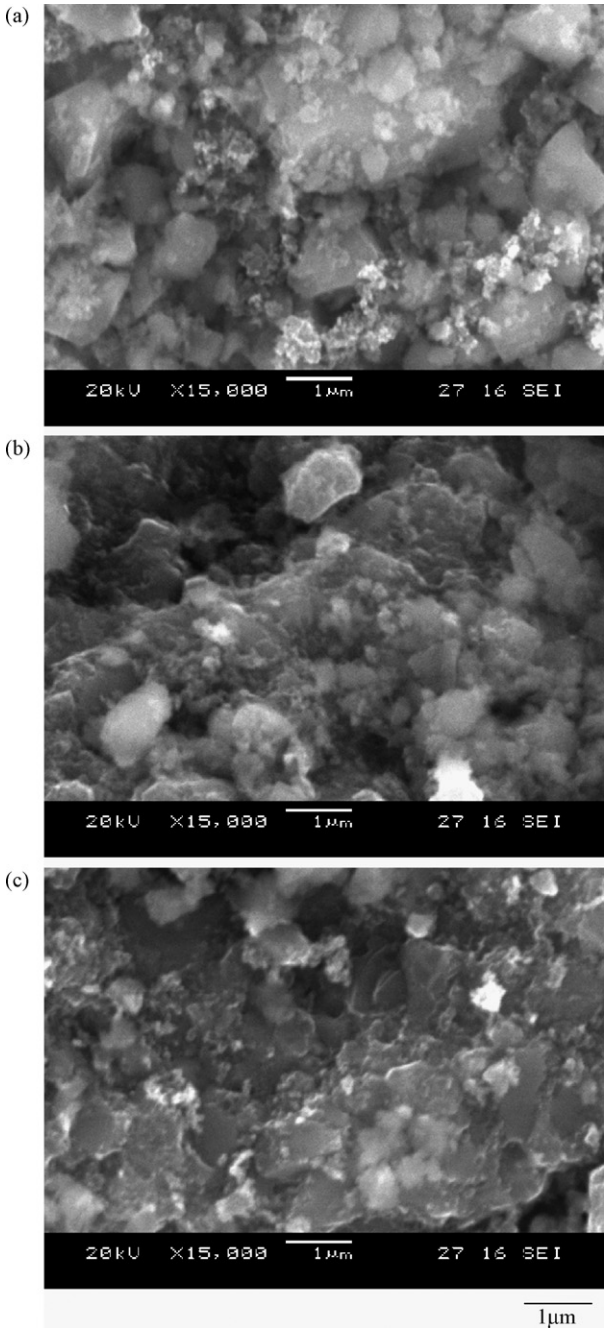

Fig. 4. Magnified SEM images of (a) the Li_2S + C blended powder and the SPS-treated ((b) at 600 °C and (c) 1000 °C) Li_2S–C composites. Magnification is the same for each micrograph.

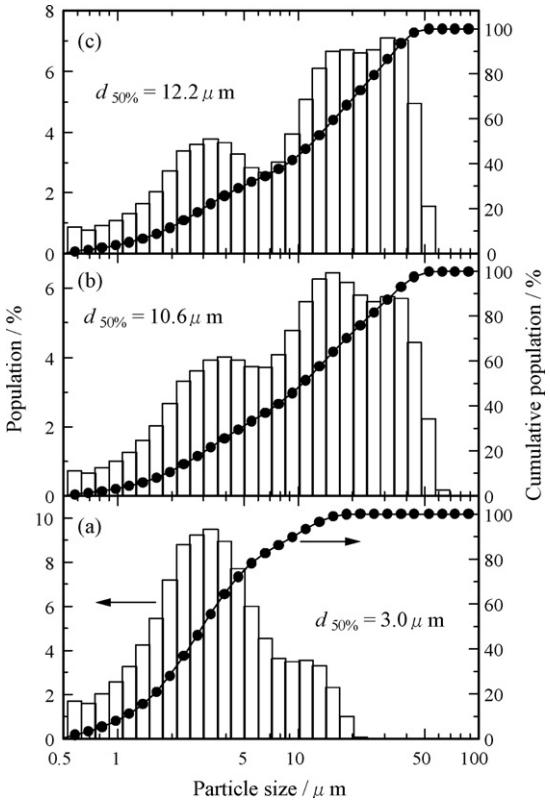

Fig. 5. Particle size distribution measured by laser diffraction and scattering method for (a) the Li_2S + C blended powder and the SPS-treated ((b) at 600 °C and (c) 1000 °C) Li_2S–C composites. The average particles size is represented by the value at 50% cumulative population ($d_{50\%}$).

Slightly larger $d_{50\%}$ value of the 1000 °C-treated SPS composite, as compared with the 600 °C-treated sample, would be originated from the presence of more amounts of larger particles of >30 μm, which were growingly formed at higher SPS temperature. Although the presence of agglomerated particles usually reduces the tap density, the present SPS-treated composites showed relatively higher tap density; it increased from *ca.* 0.40(3) g cm^{-3} (Li_2S + C blended powder) to *ca.* 0.57(3)–0.64(3) g cm^{-3} (Li_2S–C composites) by the SPS treatment. This again suggests the formation of strong binding between the Li_2S and carbon powders by the SPS treatment, since the tap density is a parameter showing how much the connections among the active materials and carbon powder are formed [13–15]. Such improved tap density would be advantageous for preparing higher density electrodes. Thus, the densification and the carbon contacts to Li_2S were simultaneously achieved by the present SPS treatment, though the carbon composites usually reduce the tap density due to the bulky volume of carbon [10].

Fig. 6 shows the initial and 10th charge and discharge curves for the cells with the SPS-treated Li_2S–C composites. Notably the SPS-treated composite sample cells showed the initial charge capacities of 450–1290 mAh g^{-1}, though Li_2S has been reported to show no significant charge capacities when conventionally mixed with carbon powder [4,7]. We also carried out the electrochemical tests for the Li_2S + C blended powder and confirmed that the initial charge capacities were less than 1 mAh g^{-1}. These results indicate that the Li_2S was activated by the strong connections to carbon powders, formed by the SPS process. Such strong connections to carbon powders were also suggested by the impedance measurements. Fig. 7 shows the Nyquist plots for the cells with the SPS-treated (at 600 °C) Li_2S–C composite samples and the Li_2S + C blended powder after fully charging. Both plots consisted of mainly the specific semi-circles and the low-frequency spikes, and the small tails were noticeable at higher frequency region. The size of the specific semi-circle decreased significantly after the SPS treatment, while the high-frequency tail remained nearly unchanged. According to the previous reports [19,20], the specific semi-circles and the high-frequency tails can be assigned to the interfacial resistances in the cathode and anode, respectively. Therefore, these results suggest that the interfacial resistance of Li_2S was much reduced by the SPS treatment, due to the formation of strong binding between Li_2S and carbon powders.

In Fig. 6, the charge capacity showed the maximum value for the 600 °C-treated sample cells, which might be due to less amounts of impurity (Li_2CO_3 and Li_2O) and less lithium deficiency in the Li_2S–C composites, as described above. A notable point is that

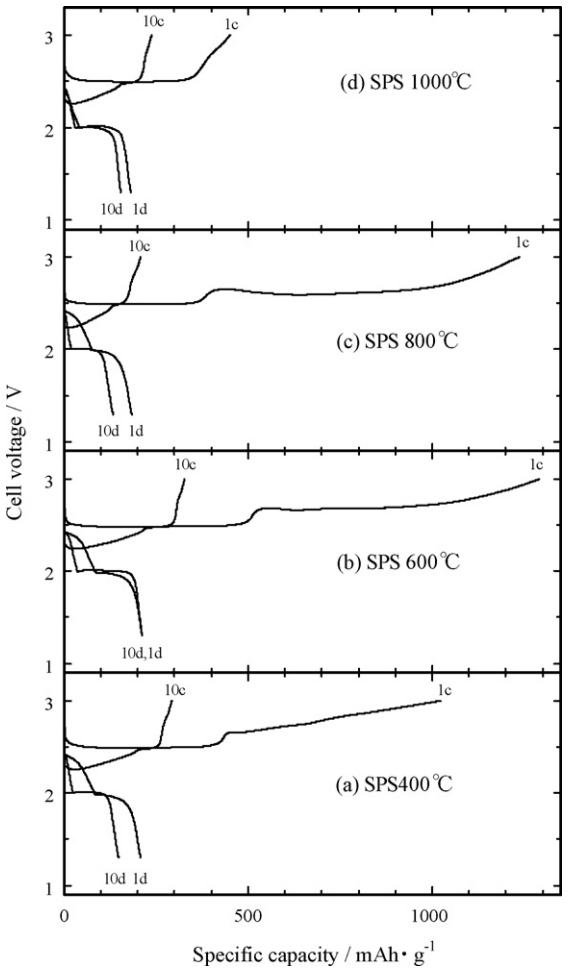

Fig. 6. Initial and 10th charge and discharge profiles for the SPS-treated ((a) at 400, (b) 600, (c) 800, and (d) 1000 °C) Li_2S–C composite sample cells at 46.7 mA g^{-1} (0.04*C*).

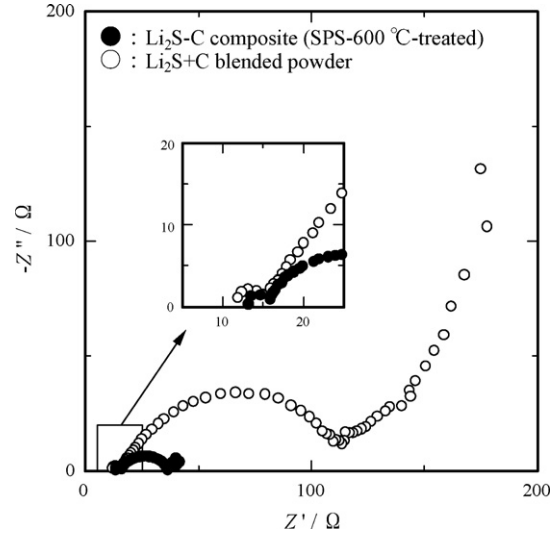

Fig. 7. Nyquist plots for the cells with the Li_2S+C blended powder and the SPS-treated (at 600 °C) Li_2S–C composite samples after fully charging.

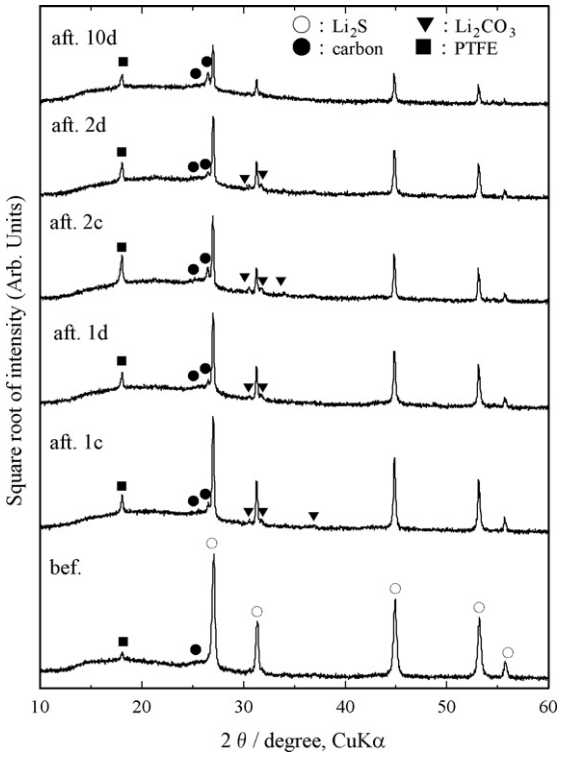

Fig. 8. *Ex situ* XRD patterns for the 600 °C-treated Li_2S–C composite positive electrodes before electrochemical test and after the first, second, and 10th cycling.

the initial charge capacity of the 600 °C-treated sample cells (*ca.* 1290 mAh g^{-1}) was beyond the theoretical capacity of Li_2S (*ca.* 1170 mAh g^{-1}). This indicates that the excess charge current was consumed by an "irregular" electrochemical reaction, such that soluble polysulfides Li_2S_x ($x \geqq 4$) are formed and they migrate to the negative electrode and are reduced there, as observed in the overcharging behavior for the Li/S cells [2]. In spite of the large values and the variation of the initial charge capacities, the discharge capacities showed relatively low and similar values (*ca.* 180–210 mAh g^{-1}) irrespective of the SPS temperature. The two plateaus in the discharge curves (*ca.* 2.4 and 2.0 V) were similar to those in the Li/S cells, where the reduction of elemental sulfur to form soluble polysulfides occurs in the 2.4–2.1 V region and the soluble polysulfides are reduced to form the solid-state Li_2S in the 2.1–1.5 V region [3]. In the following cycling, the charge capacity degraded very rapidly, but the discharge capacity remained rather comparable or somewhat reduced to the initial value; the capacity retentions after 10 cycles were *ca.* 70–100%.

In order to examine the structural changes of Li_2S during electrochemical cycling, we disassembled the 600 °C-treated Li_2S–C composite sample cells after cycling, washed the positive electrodes with TEGDME to remove the electrolyte, and carried out the XRD measurements. Fig. 8 shows the *ex situ* XRD patterns for the initial positive electrode and those after the first, second, and 10th cycling. In the first charge, the Li_2S was still remained, and any peaks ascribed to elemental sulfur, which were anticipated to appear assuming an ideal electrochemical reaction $Li_2S \rightarrow 2Li + S$, were not detected. No detection of elemental sulfur and remaining of Li_2S even at 100% depth of charge were also reported for the Li/S cells [3]. This indicates that the initial Li_2S was not fully utilized in the first charge, though its capacity was beyond the theoretical value of Li_2S. Therefore, major parts of the charge current were consumed by an "irregular" electrochemical reaction, as described above. In the following discharge, again any peaks other than Li_2S were not detected. These XRD patterns during charge/discharge

were repeated in the following cycling. Some small peaks, assigned to Li_2CO_3, were detected infrequently in the sample electrodes, which would be formed by the reaction with trace amounts of air, owning to the incomplete sealing of the sample electrodes during the XRD measurements.

Based on the above results, the following electrochemical behaviors are suggested for the present Li/Li_2S–C cells; in the first charge, some amounts of Li_2S were converted to soluble polysulfides, and they migrated to the negative electrode and were reduced there. Excess charge current was consumed for such "irregular" electrochemical reaction, and some amounts of Li_2S were remained unchanged in the positive electrode. The soluble polysulfides were hardly oxidized to the solid-state elemental sulfur in the positive electrode. In the following discharge, some of the reduced polysulfides in the negative electrode were oxidized to soluble polysulfides in the 2.4–2.1 V region. Then, they migrated back to the positive electrode and were reduced there to form the solid-state Li_2S in the 2.1–1.5 V region. Relatively low discharge capacity values as compared with the preceding charge capacity values suggest that the above-mentioned discharge reactions proceeded incompletely; the reduced polysulfides in the negative electrode partly remained unchanged, or soluble polysulfides in the electrolyte were not reduced wholly to form the solid-state Li_2S. In the following cycling, the above "shuttle mechanism" was repeated, but the irreversible polysulfides would be deposited increasingly in the negative electrode, or soluble polysulfides would be concentrated in the electrolyte, which would be responsible for the capacity degradation with cycling.

One more notable point in Fig. 8 is that the intensity of the XRD peaks ascribed to Li_2S was reduced with the electrochemical cycling. This suggests the loss of the active material into the electrolyte as a form of soluble polysulfides during the redox cycling; as described above, some amounts of Li_2S were converted to soluble polysulfides when charging, and they were not wholly reformed to Li_2S when discharging. The loss of the active material is also suggested by the morphological changes of the sample electrodes, as shown in Fig. 9. After the initial cycle, there observed several small humps in the electrodes, which were formed when sulfur-based active materials were dissolved into electrolytes [21]. Some small cracks might be formed accompanying with the dissolution of Li_2S. After 10 cycles, these humps and cracks were extended, suggesting that the active material was progressively dissolved into the electrolyte with cycling. This is consistent with the low peak intensity in the XRD patterns (aft. 10d in Fig. 8). Such progressive dissolution would contribute to retain the discharge capacity of the cells, because it would supply enough polysulfides that were returned back to the positive electrode and reduced there to reform the solid-state Li_2S when discharging. The relatively higher capacity retention of the sample cells (*ca.* 100% after 10 cycles, Fig. 6(b)) indicates that the active material was effectively dissolved to supply polysulfides enough to maintain the similar discharge capacity value.

Although the soluble polysulfides seemed to be formed in the first charge, as described above, they might be partly formed during the SPS process. As shown in Figs. 1 and 2, the disappearance of Li_2O (or $LiOH{\cdot}H_2O$), which might result in the oxidation of Li_2S, and the Li deficiency (particularly at higher SPS temperatures, >800 °C) suggest the formation of soluble polysulfides Li_2S_x ($x \geqq 4$). The relatively lower charge capacity for the SPS-1000 °C-treated sample cells, Fig. 6(d), might suggest that the presence of pre-formed polysulfides reduced the excess charge current necessary for the formation of polysulfides. Similar discharge capacities irrespective of the variety of charge capacities, Fig. 6, suggest the solubility limit of polysulfides, which was dependent on the liquid electrolyte.

According to the present results, enhancement of the electrical conductivity is required for further improvement of the utilization of Li_2S active materials. Therefore, adding further amounts of carbon might be effective for improving the capacity values. We then prepared the SPS-treated (at 600 °C) Li_2S–C composites with a weight ratio of Li_2S:AB = 5:5 and carried out the electrochemical tests. As shown in Fig. 10, the discharge capacity was enlarged (*ca.* 380 mAh g^{-1}) nearly twice of the above Li_2S–C (8:2) composites, and it showed a good cycle performance; the capacity retention after 10 cycles was *ca.* 94%. Although this improvement was mainly due to the increase in the amounts of the activated Li_2S particles connected strongly to more amounts of AB powder, some other effect, such that the additive carbon acts as absorbing the polysulfides to avoid their dissolution into the electrolytes, might contribute to it, as is observed in the cells with S–C (mesoporous carbon) composites [8]. For further improvement of the discharge

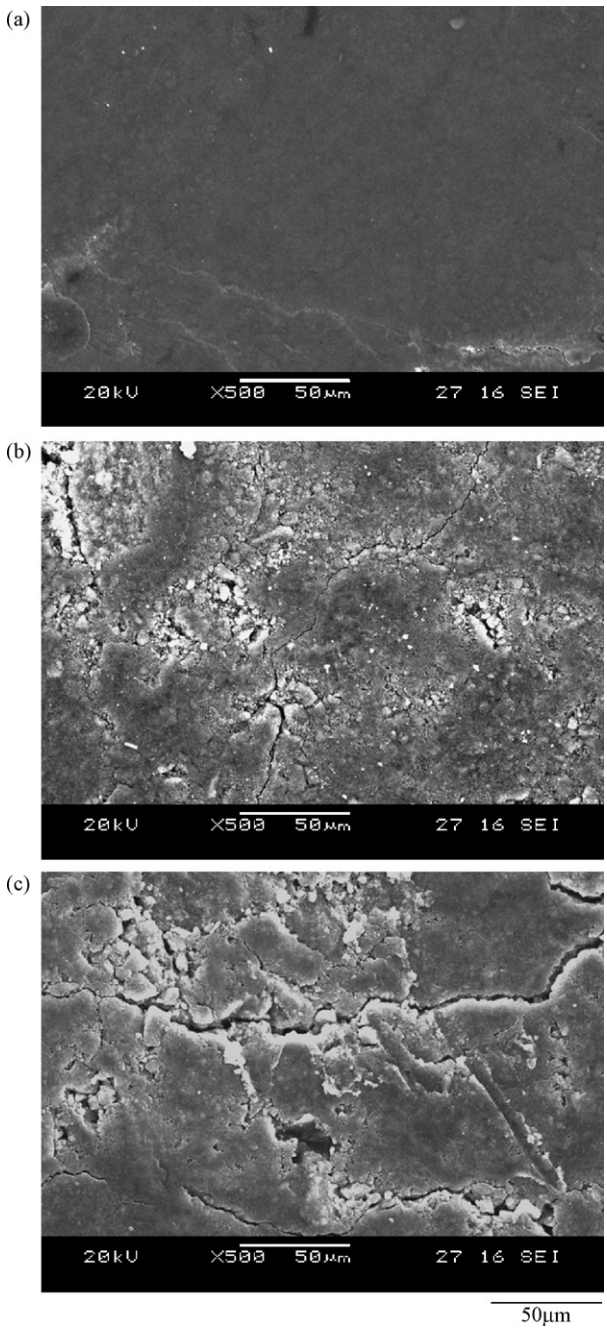

Fig. 9. SEM images for the SPS-treated (at 600 °C) Li_2S–C composite electrodes (a) before electrochemical tests, and after (b) the initial and (c) the 10th discharge. Magnification is the same for each micrograph.

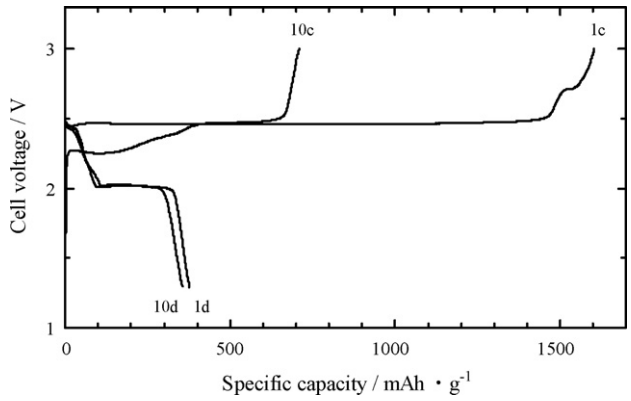

Fig. 10. Initial and 10th charge and discharge profiles for the cells with the SPS-treated (at 600 °C) Li_2S–C composite sample (weight ratio of Li_2S:C = 5:5) at 46.7 mA g^{-1} (0.04*C*).

capacity, optimization of the electrolytes seems necessary, and we are currently underway for modifying the electrolytes to be suitable for the Li_2S–C composite electrodes.

4. Conclusions

We have successfully prepared the electrochemically active Li_2S–C composites using the SPS process. The electrochemical tests demonstrated that the SPS-treated Li_2S–C composites showed the initial charge and discharge capacities of *ca.* 1200 and 200 mAh g^{-1}, respectively, though Li_2S has been reported to show no significant charge capacities when conventionally mixed with carbon powder. Such activation of Li_2S was attributed principally to strong bindings between Li_2S and carbon powders, formed by the SPS treatment. The charge/discharge behavior would take place partly by a "shuttle mechanism" similar to the Li/S cells.

Acknowledgments

We thank Dr. Hikaru Sano and Dr. Hirofumi Yamamoto of National Institute of Advanced Industrial Science and Technology (AIST) for their help with the SEM observations. Part of this work was financially supported by R&D project for Li batteries by METI and NEDO.

References

[1] D. Marmorstein, T.H. Yu, K.A. Striebel, F.R. McLarnon, J. Hou, E.J. Cairns, J. Power Sources 89 (2000) 219.
[2] J. Shim, K.A. Striebel, E.J. Cairns, J. Electrochem. Soc. 149 (2002) A1321.
[3] S.-E. Cheon, K.-S. Ko, J.-H. Cho, S.-W. Kim, E.-Y. Chin, H.-T. Kim, J. Electrochem. Soc. 150 (2003) A796.
[4] M.N. Obrovac, J.R. Dahn, Electrochem. Solid-State Lett. 5 (2002) A70.
[5] T. Kobayashi, Y. Imade, D. Shishihara, K. Homma, M. Nagao, R. Watanabe, T. Yokoi, A. Yamada, R. Kanno, T. Tatsumi, J. Power Sources 182 (2008) 621.
[6] A. Hayashi, R. Ohtsubo, T. Ohtomo, F. Mizuno, M. Tatsumisago, J. Power Sources 183 (2008) 422.
[7] B.H. Jeon, J.H. Yeon, K.M. Kim, I.J. Chung, J. Power Sources 109 (2002) 89.
[8] X. Ji, K.T. Lee, L.F. Nazar, Nat. Mater. 8 (2009) 500.
[9] J.L. Wang, J. Yang, J.Y. Xie, N.X. Xu, Y. Li, Electrochem. Commun. 4 (2002) 499.
[10] Z. Chen, J.R. Dahn, J. Electrochem. Soc. 149 (2002) A1184.
[11] M. Tokita, J. Soc. Powder Technol. Jpn. 30 (1993) 790.
[12] Z. Shen, M. Nygren, J. Mater. Chem. 11 (2001) 204.
[13] T. Takeuchi, M. Tabuchi, A. Nakashima, T. Nakamura, Y. Miwa, H. Kageyama, K. Tatsumi, J. Power Sources 146 (2005) 575.
[14] T. Takeuchi, M. Tabuchi, A. Nakashima, H. Kageyama, K. Tatsumi, Electrochem. Solid-State Lett. 8 (2005) A195.
[15] T. Takeuchi, M. Tabuchi, K. Ado, K. Tatsumi, J. Power Sources 174 (2007) 1063.
[16] F. Izumi, T. Ikeda, Mater. Sci. Forum 321–324 (2000) 198.
[17] F. Kubel, B. Bertheville, H. Bill, Z. Kristallogr. 214 (1999) 302.
[18] A. Grzechnik, A. Vegas, K. Syassen, I. Loa, M. Hanfland, M. Jansen, J. Solid State Chem. 154 (2000) 603.
[19] G. Nagasubramanian, J. Power Sources 87 (2000) 226.
[20] J. Shim, R. Kostecki, T. Richardson, X. Song, K.A. Striebel, J. Power Sources 112 (2002) 222.
[21] S.C. Han, H.S. Kim, M.S. Song, P.S. Lee, J.Y. Lee, H.J. Ahn, J. Alloys Compd. 349 (2003) 290.